Remote Sensing of Environment 216 (2018) 735–746

Contents lists available at ScienceDirect

Remote Sensing of Environment

journal homepage: www.elsevier.com/locate/rse

Assessing the accuracy of satellite derived ocean currents by comparing observed and virtual buoys in the Greater Agulhas Region

Michael G. Hart-Davis[a,c,*], Björn C. Backeberg[b,c,d], Issufo Halo[a,c], Erik van Sebille[e], Johnny A. Johannessen[d,f]

[a] Department of Conservation and Marine Sciences, Cape Peninsula University of Technology, Cape Town, South Africa
[b] Council for Scientific and Industrial Research, Natural Resources and the Environment, Coastal Systems Research Group, Stellenbosch, South Africa
[c] Nansen-Tutu Centre for Marine Environmental Research, Department of Oceanography, University of Cape Town, South Africa
[d] Nansen Environmental and Remote Sensing Center, Bergen, Norway
[e] Institute for Marine and Atmospheric Research, Department of Physics, Utrecht University, Netherlands
[f] Geophysical Institute, University of Bergen, Norway

ARTICLE INFO

Keywords:
Synthetic particle tracking
GlobCurrent
Surface drifting buoys
The Greater Agulhas Current System

ABSTRACT

In this study, we assess the accuracy of a combined geostrophic and Ekman current product (GlobCurrent) that estimates ocean currents at 15 m depth, by coupling it to a synthetic particle tracking tool and comparing the virtual trajectories to those of surface drifting buoys drogued at 15 m in the Greater Agulhas Current Region. The velocities from a total of 1041 drifters are compared and evaluated to the synthetic particle-derived velocities for the period 1993–2015. On average the GlobCurrent underestimates the velocity in the Greater Agulhas Current by approximately 27%. The underestimation ranges from 4 to 64% in different regions, with the smallest error found in the Agulhas retroflection region, and the highest in the Benguela Upwelling System. Furthermore, we compare the time taken for the separation between the virtual and real drifters to reach 35 km. The mean separation time was found to be 78 h, with the shortest time (35 h) found in the Agulhas Current and the longest time (116 h) located in the Agulhas Return Current. Deploying 10,000 virtual drifters in a 1° × 1° box within the southern Agulhas Current shows a convergence of trajectories towards the core of the current, while higher divergence is evident in the Agulhas retroflection. To evaluate the utility of this synthetic particle tracking tool coupled with GlobCurrent in open ocean search and rescue operations, two test cases are examined: (1) a capsized catamaran spotted south of Cape Recife and recovered 5 days later south of Cape Agulhas; and (2) a drifter trajectory in the same region. The comparison suggests that the GlobCurrent forced synthetic particle tracking tool is not appropriate for predicting the trajectory of a capsized catamaran that does not have the same drift characteristics as a surface drifting buoy drogued to 15 m.

1. Introduction

The Greater Agulhas Current is one of the most energetic western boundary current systems in the world, and plays a fundamental role in the regional marine environment, the regional weather as well as global climate (Beal et al., 2011) (Fig. 1). It influences the oceanography of coastal and shelf regions through a range of mesoscale (~50–200 km) and submesoscale (< 10 km) processes, such as eddy shedding, plumes, filaments, and the intrusion of the current onto the shelf (Lutjeharms, 2006; Krug et al., 2014). The Agulhas Current is one of the fastest flowing western boundary currents with mean maximum velocities of about 1.5 m/s, often reaching speeds > 2 m/s (Rouault et al., 2010). The Agulhas Current and the South-East Madagascar Current are separated by the Mozambique Basin, which is characterized by intense mesoscale activity (Halo et al., 2014a). The transports within the South-East Madagascar Current and through the Mozambique Channel (Halo et al., 2014b) are important sources of the flow of the Agulhas Current (Halo et al., 2014a; Backeberg et al., 2008).

The Agulhas Current is divided into two different parts, the southern and northern Agulhas Current, which exhibit distinct differences in path characteristics (Lutjeharms et al., 2003). The path of the northern Agulhas is considered to be unusually stable for a western boundary current (Gründlingh, 1983) as the current is steered along a narrow shelf with a steep slope, with typical annual velocities ranging from

* Corresponding author at: Nansen-Tutu Centre for Marine Environmental Research, Department of Oceanography, University of Cape Town, Rondebosch, Cape Town, 7700, South Africa.
E-mail address: mhartd@gmail.com (M.G. Hart-Davis).

https://doi.org/10.1016/j.rse.2018.03.040
Received 31 August 2017; Received in revised form 27 February 2018; Accepted 29 March 2018
Available online 07 April 2018
0034-4257/

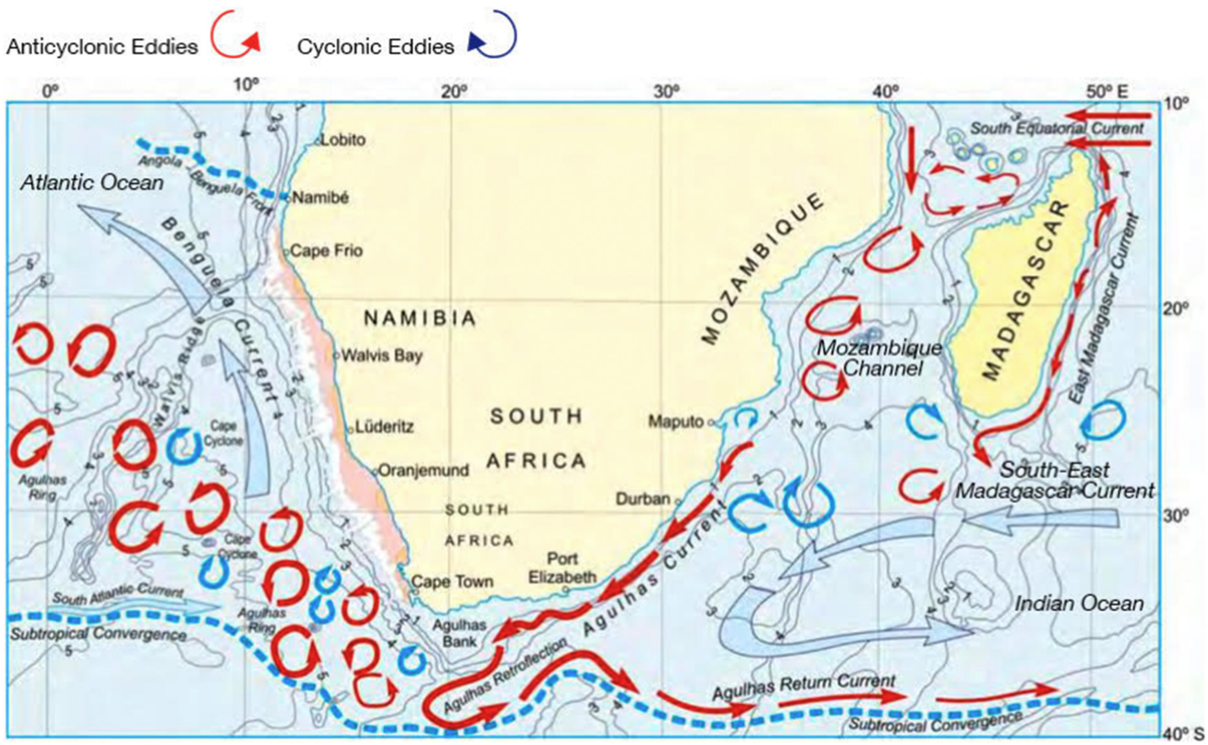

Fig. 1. An illustration of the flow of the currents around the coast of southern Africa, including the Agulhas Current, the Benguela Current, East Madagascar Current and the Agulhas Return Current (Ansorge and Lutjeharms, 2007).

1.4 m/s to 1.6 m/s (Lutjeharms, 2006). In contrast, the southern Agulhas Current displays large meanders (Harris et al., 1978) due to weakening of the topographic steering (De Ruijter et al., 1999; Lutjeharms, 2006). The mean annual surface velocities in the southern Agulhas Current range between 1.5 m/s and 2.0 m/s (Lutjeharms, 2006). The meanders and perturbations on the near shore boundary of the current are known to contribute to the intensification of the thermocline on the Agulhas Bank through the input of warmer water (Rouault et al., 2010).

South of the Agulhas Bank (at approximately 36°S), the Agulhas Current begins to turn eastward in an anticyclonic loop known as the Agulhas Retroflection (Duncombe Rae, 1991). The retroflection contains some of the highest levels of mesoscale variability in the world's ocean (Garzoli et al., 1996) and is associated with the formation and shedding of large anticyclonic eddies known as Agulhas Rings (Lutjeharms and van Ballegooyen, 1988; De Ruijter et al., 1999). The Agulhas Rings transport warm, salty water into the South Atlantic Ocean in a process known as the Agulhas leakage (Van Leeuwen et al., 2000; Backeberg et al., 2008).

The majority of the Agulhas Current flows back into the South Indian Ocean as the Agulhas Return Current and is characterized with strong mesoscale variability as a result of recurrent eddy generation (Lutjeharms and Ansorge, 2001; Lutjeharms and Valentine, 1988). Its core width is around 70 km wide and it has a mean velocity that reaches up to 2 m/s (Backeberg et al., 2008).

The west coast of southern Africa is dominated by the Benguela Upwelling System. The Benguela Upwelling System is a highly productive region due to the upwelling that takes place near the coast of southern Africa (Van der Lingen et al., 2006). Substantial mesoscale activity in the form of eddies and filaments are a constant feature of the Benguela Upwelling System (Blanke et al., 2002) which impacts the ecosystem dynamics and cross-slope exchanges between the coastal upwelling system and the open ocean (Rubio et al., 2009). The shedding of cyclonic eddies off the coast of Cape Columbine and the frequent Agulhas Rings that originate from the Agulhas Retroflection are the main sources of mesoscale activity in this region (Hardman-Mountford et al., 2003). Advances in the understanding, monitoring and forecasting of the intense dynamic variability of the ocean currents surrounding southern Africa is challenging but represents a direct benefit to the industrial, commercial and leisure activities, including the monitoring of accidental pollutants, such as oil spills as well as harmful algal blooms.

Scientists have developed many techniques to increase the understanding of upper ocean currents including the use of Acoustic Doppler Current Profilers, Radio Detecting and Ranging systems (HF-radar) and the deployment of surface drifters. Surface drifters have been extensively used to study the ocean currents (Brambilla and Talley, 2006; McClean et al., 2002) and used in combination with ocean currents derived from satellites and ocean models, to provide a powerful means to monitor and forecast the ocean surface currents.

Synthetic particle tracking tools have been introduced and used to investigate the ocean dynamics predicted by ocean models (Hidalgo et al., 2009; Biastoch et al., 2015; Xu et al., 2016). Lagrangian synthetic particle tracking tools have also been developed to study a wide range of ocean processes and have a variety of applications (Fredj et al., 2016; Van Sebille et al., 2018) including larval dispersion (Thorpe et al., 2004), oil spills (Sayol et al., 2013), hydrodynamic connectivity (Van Sebille et al., 2010) and search and rescue.

In this paper, we investigate the use of a synthetic particle tracking tool in assessing the accuracy of a recently released global ocean current product (http://www.globcurrent.org) derived from combined geostrophic and Ekman current estimates. Virtual trajectories derived from the tracking tool are compared to those observed from surface drifting buoys drogued to 15 m. The level of agreement is addressed in the context of strength and weaknesses in the GlobCurrent-based products related to the inherent spatial and temporal resolution of the dominant processes and dynamics in this highly complex Greater Agulhas Current regime. The paper is structured as follows: Section 2 describes the surface drifter observations, the GlobCurrent ocean current product used, the synthetic particle tracking tool and the simulations run. In Section 3 the comparisons between the virtual and real drifter trajectories are presented and discussed. In Section 4 the synthetic particle tracking tool is applied and assessed in a search and rescue application. The major findings are summarized and concluded in Section 5.

2. Data and methods

2.1. Surface drifter observations

As part of the global drifter programme (GDP), surface drifters drogued at 15 m depths are deployed throughout the global oceans (Lumpkin et al., 2013). The GDP provides comprehensive in-situ observations of ocean surface temperatures and currents (Hansen and Poulain, 1996) that together with drifter positions are transmitted via the Argos satellite system (Brambilla and Talley, 2006). The Global Drifter Centre at the Atlantic Oceanographical and Meteorological Laboratory (AOML) stores the raw data, applies quality control procedures and interpolates the data into hourly (Elipot et al., 2016) or 6-hourly intervals and calculates the velocities (Lumpkin and Pazos, 2005).

In this project, we examine 1041 drifters deployed in the domain defined as 2°W–70°E and 5–52°S from 1993 to 2015 (Fig. 2a). The chosen domain encompasses the Mozambique Channel and its mesoscale eddies; the Southern Extension of the East Madagascar Current; the Agulhas Current including the retroflection region with eddy shedding; the Benguela Upwelling System; and the Agulhas Return Current including the northern limit of the Southern Ocean (Fig. 2b). The chosen domain is one of the most dynamic and variable regions in the world which offers an opportunity to evaluate the GlobCurrent product for a variety of ocean processes and dynamics with different spatial-temporal characteristics, facilitating a comparison of the regional different currents and processes.

Several oceanographic research lines have been conducted over the years in the open ocean around the South African coastline. The approximate geographical location of the lines can be discerned in Fig. 2 along which drifter deployments are seen to be clustered. Examples include the Crossroads line (from approximately 47°S and 31°E to Cape Town) (Morris et al., 2017), the GoodHope line (from Cape Town to 0°E and 52°S) (Speich et al., 2012) and the SAMBA line (along 34.5°S towards South America) (Ansorge et al., 2014). The mean duration of all drifters' trajectories in the chosen domain is 137 days, with the longest drifter trajectory lasting 1491 days and the shortest being one day. Only drifters that were deployed in the defined domain during the period 1993–2015 were considered in the analysis, overlapping with the satellite altimetry data. Drifters that collected data for less than one day were removed from the analysis. Additionally, only drifters that still had their drogues intact were considered and any undrogued drifters were removed from this project.

2.2. GlobCurrent ocean velocities

Based on a satellite sensor synergy and analysis approach the GlobCurrent project (Johannessen et al., 2016) has delivered surface current products collocated with the sea surface temperature field. Multi-satellite altimetry from 1993 to 2015 is used to provide daily estimates of surface geostrophic currents for the global ocean at a spatial resolution of 25 km (http://www.globcurrent.org). The geostrophic currents are obtained by merging data from multiple altimeter missions with gravity models and in-situ data into a gridded product of absolute dynamic topography, which is the sum of the sea level anomalies and the mean dynamic topography (Rio et al., 2014). This product is combined with 3-hourly Ekman currents (at surface and 15 m depth) estimated from drogued surface drifter data, Argo floats and near surface winds.

The use of drogued drifters in GlobCurrent is only to help compute synthetic estimates of the mean dynamic topography as well as the mean geostrophic current and Ekman current. Therefore, drifter data can be used to validate the GlobCurrent product as the estimates of surface ocean currents by GlobCurrent are not directly made from the drifter data.

The u- and v-components of the geostrophic velocity are defined as follows (Saraceno et al., 2008):

$$\upsilon_{geo} = -\left(\frac{g}{f}\right)\cdot\frac{\delta\eta}{\delta y} \tag{1}$$

$$\nu_{geo} = \left(\frac{g}{f}\right)\cdot\frac{\delta\eta}{\delta x} \tag{2}$$

where υ represents the zonal component, ν the meridional component,

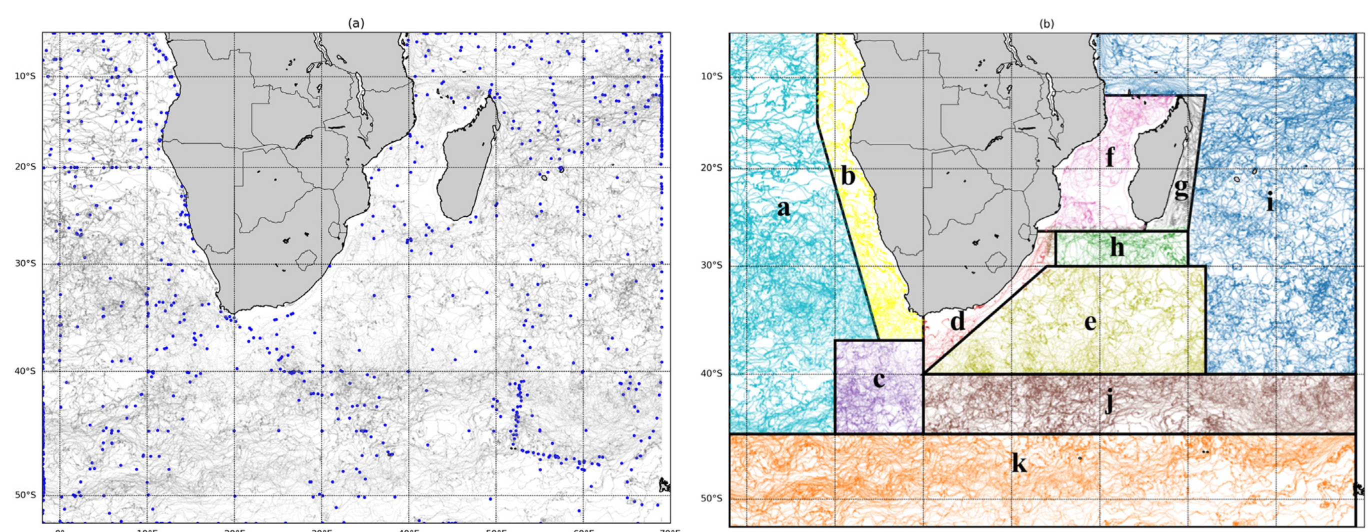

Fig. 2. (a) The starting locations (blue dots) and trajectories (grey lines) of all the GDP drifters deployed within the domain between 1993 and 2015. (b) An illustration of the sub-regions of the study that are defined as follows: a – South-East Atlantic Ocean, b – Benguela Upwelling System, c – Agulhas Retroflection, d – Agulhas Current, e – Agulhas Return Current Recirculation, f – Mozambique Channel, g – East Madagascar Current, h – South-East Madagascan Current, i – South-West Indian Ocean, j – Agulhas Return Current and k – Southern Ocean. (For interpretation of the references to colour in this figure legend, the reader is referred to the web version of this article.)

$\delta\eta$ is the variation in the sea surface height, δx and δy the distance between grid points, g the gravitational acceleration and f the Coriolis force.

The Ekman currents are estimated using the Argo floats and drifter data together with the wind stress from the European Centre for Medium-Range Weather Forecasts (ECMWF) (Rio et al., 2014). At depth z (0 m and 15 m), the relationship of the Ekman current ($\vec{v}_{ek}$) to the wind stress ($\vec{\tau}$) is expressed by:

$$\vec{v}_{ek}(z) = \beta(z).\ \vec{\tau}.\ e^{i\theta(z)} \tag{3}$$

where the β and θ coefficients at z = 0 m and z = 15 m are estimated from a least square fit between the Ekman current (e.g. respectively the geostrophic current subtracted from the Argo surface drift and the geostrophic current subtracted from the 15 m drogued drifters) and the wind stress (Rio et al., 2014).

2.3. Virtual drifters

Particle tracking is the observation of the motion of an individual particle within a fluid. Particle tracking uses a Lagrangian modelling framework that moves with the flow of the ocean and is particle specific instead of being point specific (MacDonald et al., 2006). Synthetic drifters were deployed using the GlobCurrent combined currents at 15 m depth (the zonal (u) component and the meridional (v) component) to simulate trajectories that, in turn, are compared with the surface drifter observations. A Lagrangian particle tracker known as Parcels ("Probably A Really Computationally Efficient Lagrangian Simulator") (Lange and van Sebille, 2017) was used for the simulation. Parcels is a synthetic particle tracking tool aimed at exploring novel approaches for Lagrangian tracking of virtual ocean particles (Lange and van Sebille, 2017). Parcel requires velocity data to force the synthetic particles and computes the Lagrangian trajectories of synthetic particles by using the following equation:

$$X(t + \Delta t) = X(t) + \int_{t}^{t+\Delta t} v(x, \tau) d\tau \tag{4}$$

where X is the position of the particle and v (x, τ) is the Eulerian velocity field, which equals to the Lagrangian velocity when evaluated at $X(t) = x$ (Van Sebille et al., 2018).

The starting points, dates and lengths of each surface drifter trajectory from the interpolated GDP data were used to collocate and estimate the corresponding trajectories for every synthetic drifter. Every synthetic particle (virtual drifter) was then allowed to drift for the same duration as the observed drifter, making a total of 1041 trajectory simulations between 1993 and 2015.

3. Comparing virtual and real trajectories

In this section, pairs of virtual and observed drifter trajectories are analysed in terms of speed and deformation. In so doing the ability of the GlobCurrent-based products to resolve dominant upper ocean processes and dynamics is investigated and assessed.

The real and virtual drifter trajectories for the Agulhas Current, the Benguela Upwelling System, the Mozambique Channel and the Southern Ocean are compared in Fig. 3 and reveal variable levels of agreement. In the Agulhas Current (Fig. 3a), the observed trajectory of the drifter during the early path suggests the presence of sub-mesoscale to mesoscale variability and orbital motions.

In comparison, the trajectory of the virtual drifter displays a more direct pathway with less meandering variability and orbital motions. On the other hand, the trajectories of both the virtual and real drifter converge as they enter into the core of the Agulhas Current and continue towards the retroflection area.

However, it shall be noted that the virtual drifter passed through the core of the Agulhas Current approximately 146 days before the real drifter, as the virtual drifter encountered a more direct pathway in the early part of the drift. Hence, the real and virtual drift in the retroflection region are most likely affected by currents with different temporal and spatial variability. In turn, the trajectories and pathways are different.

The comparison of the early trajectories in both the Benguela Upwelling System and the Mozambique Channel displayed in Fig. 3b and c suggests similar disagreement. In both cases the real drifters seem to get caught in small-scale variability shortly after deployment, while the virtual drifters show no evidence of being caught in such features. In some cases, the virtual drifter and the real drifter are also moving in different directions. The trajectories representing the later stages of the drifts are also markedly different, in particular for the Mozambique Channel case where the virtual drifter remained in the channel, while the observed drifter took a pathway that brought it out of the channel and into the south-western part of the Indian Ocean. On the other hand, the trajectories displayed in the Southern Ocean (Fig. 3d) show very good agreement whereby both the virtual and observed drifters follow the same meandering pathway. The only distinct variation appears at the end of their lifespan.

All in all, these findings clearly highlight significant regional differences with the best comparable trajectories found in the core of the Agulhas Current and in the Southern Ocean. This is not surprising as better comparable drifter trajectories can be expected in topographically steered current regimes and where semi-permanent meanders are present such as respectively, the Agulhas Current and the Antarctic Circumpolar Current. The mismatch in the virtual versus observed drifter trajectories that dominates the Benguela Upwelling System and Mozambique Channel regions, on the other hand, are related to the discrepancies in the spatial and temporal variability in the currents at 15 m depth. Some of this could be attributed to the linear interpolation in space and time employed in the Parcels code. However, this effect is expected to be small; Qin et al. (2014), for example, showed that on time scales shorter than approximately a week, the temporal resolution did not very much affect the results of virtual particle trajectories in the Agulhas region.

Moreover, the estimation of the Ekman current at 15 m may be based on too simple assumptions and parameterization that disfavours the comparison of the virtual drifter trajectories based on combined geostrophic and Ekman current at 15 m to the observed drifter trajectories.

It is also obvious that the 6-hourly temporal resolution in the observed drifter data that resolves inertial motion is not contained in the virtual drifter data since the GlobCurrent-based geostrophic current provides no diurnal variability. Finally, the spatial resolution in the drifter data is extremely fine (~100 m), in contrast to the 25 km resolution in the GlobCurrent-based products.

In order to examine the regional variations and differences between the simulations and the observations, spatial density plots were created for both the virtual and the real drifters (Fig. 4). These density plots display how the distribution of real and virtual drifters varies by dividing the domain into 1/2° grid cells. The total number of observed drifters (Fig. 4a) and virtual drifters (Fig. 4b) that passed through each of these grid cells was then calculated. The apparent low number of drifters in the Agulhas Current and the Retroflection region are found to be comparable in both distributions. The coarser spatial resolution (25 km) of the current used to advect the virtual drifters is considered to be the main reason for the discrepancies. This is supported in a recent study by Zheng et al. (2015) who found that a considerable number of eddies in the south-eastern region of the Mozambique Channel were smaller than 20 km in radius. Similarly, the southward region of the Agulhas Current is known to influence the coastal and shelf regions through submesoscale (< 10 km) processes (Krug et al., 2017; Lutjeharms, 2006; Lutjeharms et al., 2003). As such they are not properly resolving in the pathways of the virtual drifters. In turn, this implies that the virtual and observed drifters will be exposed to

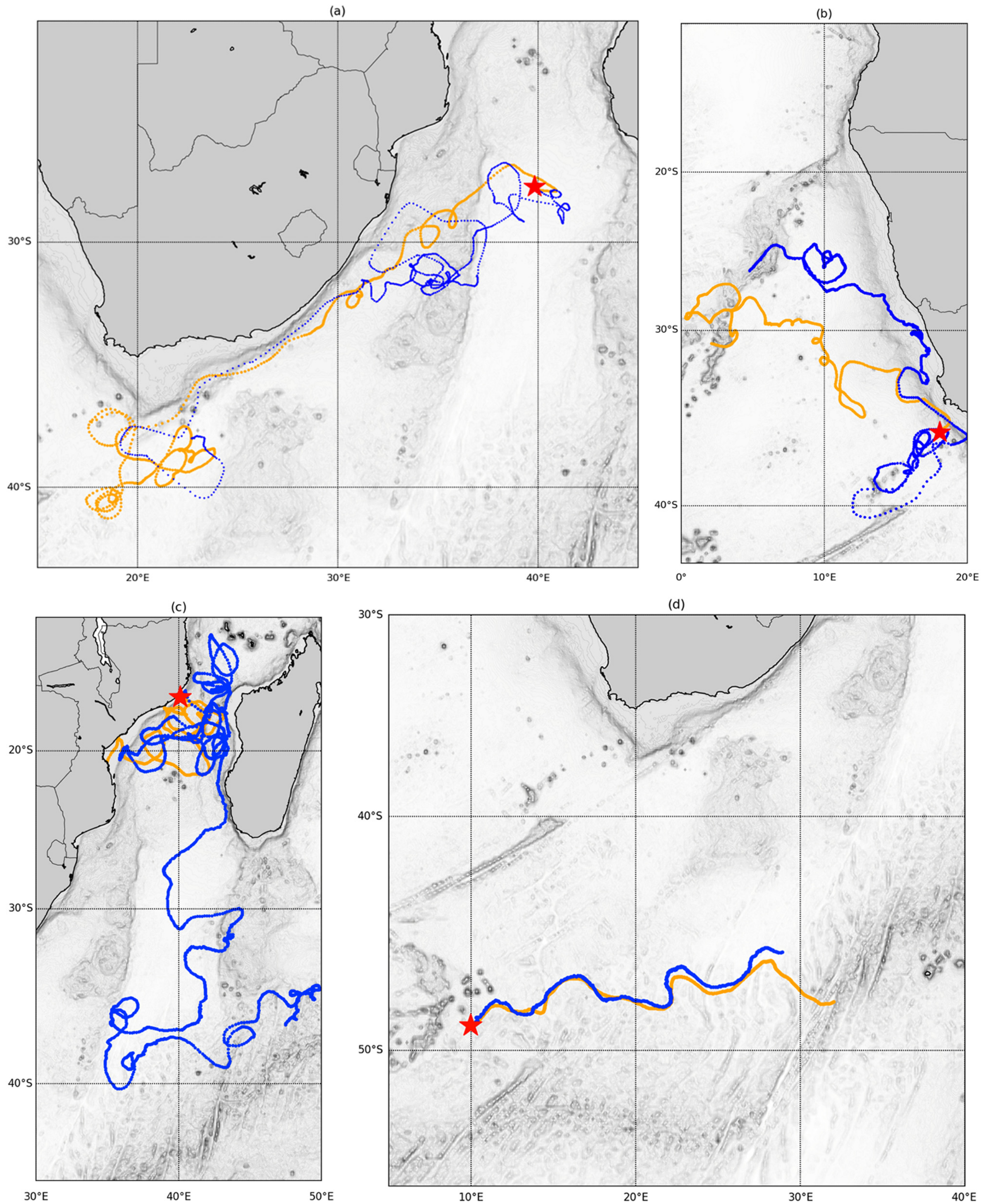

Fig. 3. Comparison of selected virtual (orange) and real drifters (blue) for: (a) the Agulhas Current, (b) the Benguela Upwelling System, (c) the Mozambique Channel and (d) the Southern Ocean. The red star represents the starting location of both the real and virtual drifter. (For interpretation of the references to colour in this figure legend, the reader is referred to the web version of this article.)

different spatial variability in the ocean current leading to the density distributions shown in Fig. 4.

Fig. 4c shows the density of real and virtual drifter trajectories that are found in each of the subdomains as well as the difference between them. Positive (negative) differences indicate that there are more (less) real drifter trajectories than virtual drifter trajectories. The distribution patterns of the real and virtual drifters show good agreement in several subdomains of the domain. The Benguela Current contains the best

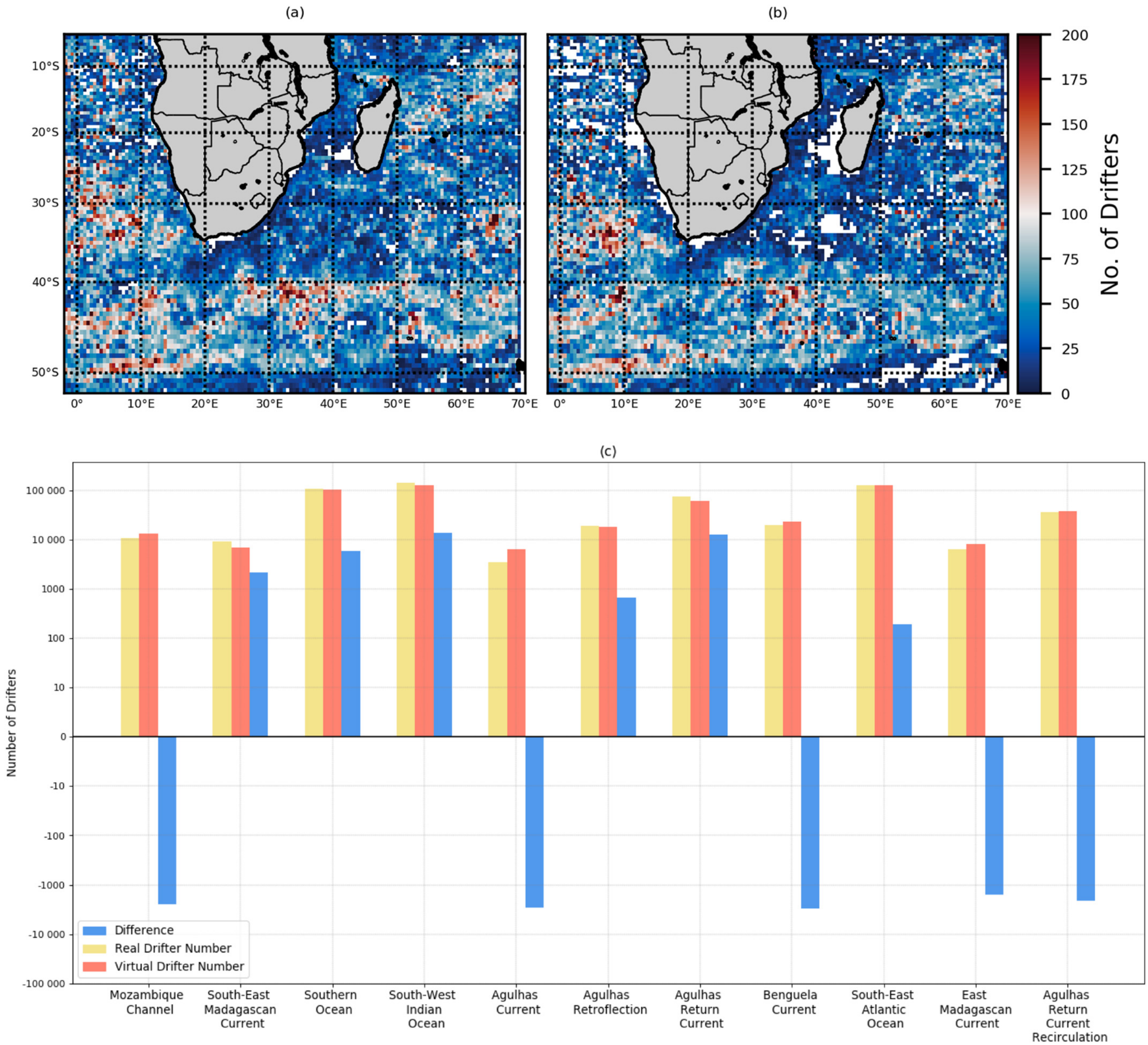

Fig. 4. Density plots indicating the number of real drifters (a) and virtual drifters (b) that pass through every 0.5° grid cell within the study area between 1993 and 2015. Grid cells with zero real or virtual drifters are indicated in white. The bar graph (c) represents the number of real (yellow) and virtual drifters (red) in all of the regions defined in Fig. 2 as well as the differences between them (blue). (For interpretation of the references to colour in this figure legend, the reader is referred to the web version of this article.)

relationship in terms drifter density of all the subdomains, with only a 10-drifter difference between observations and simulations (a 0.05% difference). Furthermore, the South-East Atlantic Ocean also showed a good relationship between drifter densities, with only a 996-drifter difference which is rather encouraging considering there were over 128,000 real drifter observations in this subdomain (a 0.77% difference). In fact, seven of the eleven subdomains showed a density difference of < 10% and none of them exceeded a difference of > 25%. The largest difference was found to be in the South-East Madagascar Current, which is supported by the study on submesoscale eddies in this region Zheng et al. (2015).

Similar to the density plots, 1/2° gridded velocity maps of the virtual and the observed drifters were created to compare the mean simulated and observed velocity within each grid cell of the entire domain from 1993 to 2015 (Fig. 5). The results reveal regions of fairly good agreement, in particular in the Agulhas Current, in the retroflection region and the Agulhas Return Current. However, the mean simulated drifter velocities are slightly lower than the observed drifter velocities. This is consistent with the findings reported by Danielson et al., (in this issue). On the other hand, the variability is distinctly larger in the observed velocities compared to the simulated virtual velocities. To further understand the differences between the velocities of the real and virtual drifters, the RMSE (Fig. 5c) was calculated. The following formula was used to calculate the RMSE:

$$RMSE = \sqrt{\sum \frac{(v_{virtual} - v_{real})^2}{N}} \tag{5}$$

where *y is* the velocity of the drifters (real and virtual) and N is the number of observations.

The RMSE for the entire domain tends to range between 0.40 and

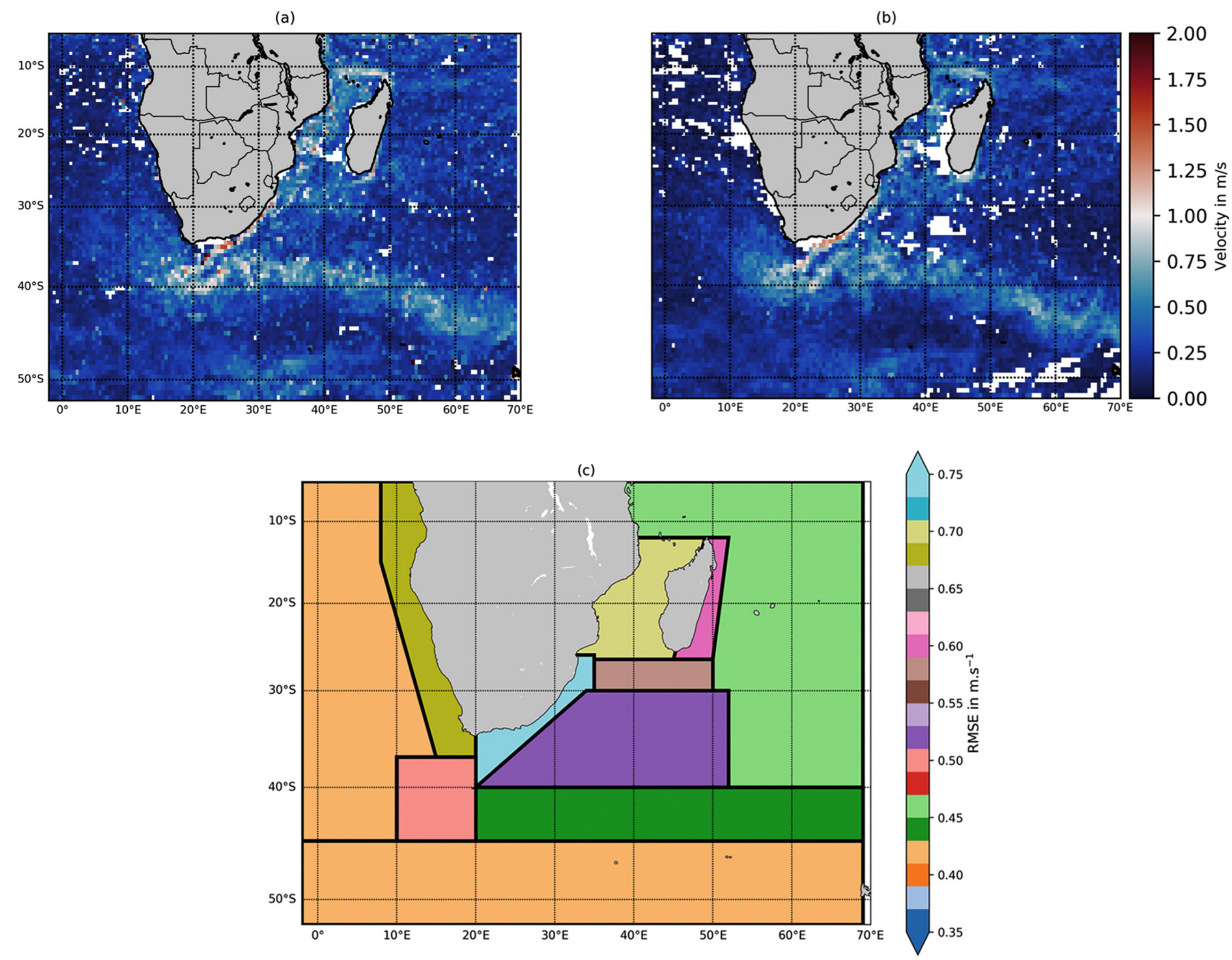

Fig. 5. The gridded (1/2°) mean velocities of real drifters (a) and virtual drifters (b) for 1993–2015. The mean velocity of each 1/2° grid cell was calculated by averaging all the velocities of all the virtual and real drifters within each grid cell. The root-mean-squared difference (RMSE) of the velocities (c) was done between the real and virtual drifters.

0.70 m/s, with the Agulhas Current (0.99 m/s) being the only subdomain that does not fall within this range. The subdomain with the lowest RMSE was the Southern Ocean (0.418 m/s), with the South-East Atlantic Ocean only having a slightly higher RMSE (0.419 m/s).

In a recent study by Meyer et al. (2017), it was reported that the GlobCurrent-based velocity field significantly underestimates the directly observed currents. This is in agreement with the results presented in Table 1. The mean velocity of all the observed surface drifters within the entire domain is 0.28 m/s compared to the GlobCurrent-based simulations with a mean of 0.22 m/s, which is a 27% drop (Table 1).

Furthermore, the histogram of the velocities for both the virtual and real drifters (Fig. 6) illustrates comparable distributions. However, the shapes vary as the simulated velocities are more narrowly distributed and shifted towards lower speeds. Region by region the underestimation varies significantly with the Benguela Upwelling System reaching the highest mean variation of 64%, the Agulhas Current of about 27% while the Agulhas Retroflection had the lowest percentage underestimation of 5%. The lower underestimation in the Agulhas Retroflection region suggests that the GlobCurrent-derived velocity field is able to capture the dominant mesoscale processes in that retroflection region.

The quantile-quantile plot (Fig. 7) further highlights the fact that the GlobCurrent-based simulations underestimate the observed surface drifter velocities for all velocities across the entire domain. On average the virtual velocities underestimate the observed velocities by 27%

Table 1
The mean velocity of all regions for both the real and the virtual drifters. The 2nd and 3rd columns represent the mean velocity of the real and virtual drifters as well as the standard deviation within each grid cell of the domain. The 4th column represents the percentage variation between the mean drifter velocity and the mean virtual drifter velocity.

Regions	Real drifter mean velocity (m/s)	Virtual drifter mean velocity (m/s)	Percentage variation between means
Domain	0.28 ± 0.45	0.22 ± 0.19	27%
Agulhas Current	0.57 ± 0.88	0.45 ± 0.37	27%
Benguela Upwelling System	0.23 ± 0.57	0.14 ± 0.12	64%
Agulhas Retroflection	0.44 ± 0.57	0.42 ± 0.27	5%
Mozambique Channel	0.46 ± 0.56	0.34 ± 0.23	35%
Agulhas Return Current	0.34 ± 0.46	0.32 ± 0.28	11%

compared. The underestimation reported in the previous studies mentioned above and further documented in this paper suggests that the GlobCurrent-derived current products that uses optimal interpolation and merging techniques to fill gaps between spatially sparse satellite data and deliver a gridded product (Ducet et al., 2000; Meyer et al.,

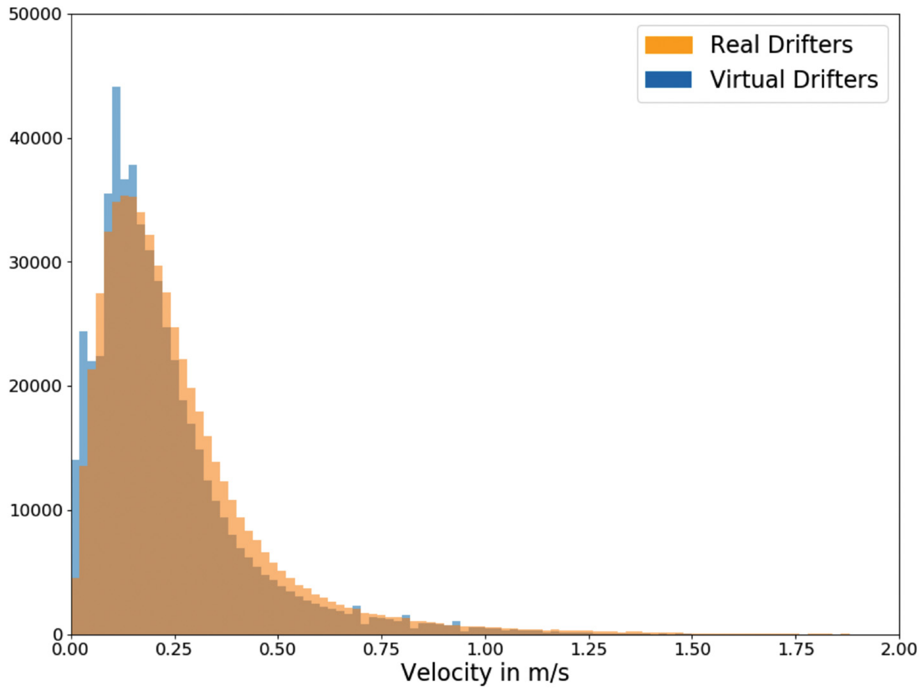

Fig. 6. Comparison of velocity histograms of real and virtual drifters for the entire domain (2°W–70°E; 5–52°S).

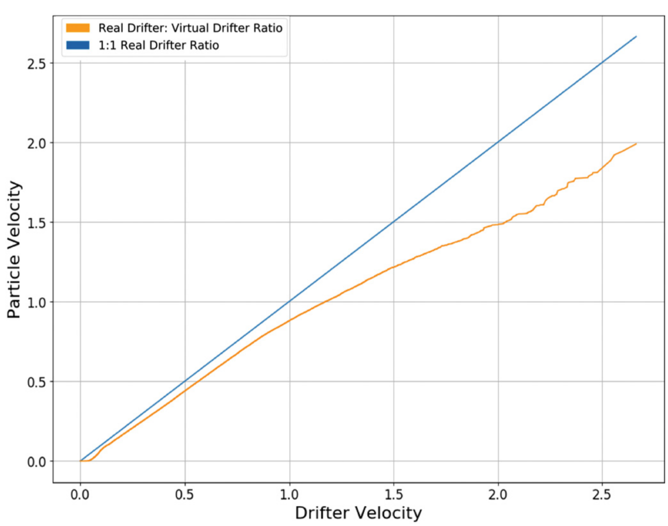

Fig. 7. Comparison of velocity quantile-quantile plots of real and virtual drifters for the entire domain (2°W–70°E; 5–52°S).

2017) result in the smoothing of data in both space and time. In turn, the ocean velocity data become underestimated. The underestimations provided by the GlobCurrent-derived forcing will result in slower moving virtual drifters, and with increasing time the virtual and the real drifters may become more and more spatially separated. Hence, they may eventually reach a separation distance that is larger than the spatial correlation wavelength. In turn, the real and virtual drifters will be exposed to different current fields and dynamic variability that may further differentiate the corresponding drifter trajectories.

As expected, the mean distance between the virtual and real drifter increases over time (Fig. 8a). This mean remains relatively low for the first 100 h of the study, after which the deviation begins to increase drastically. Applying simple trigonometry regarding the $25 * 25$ km grid cell size the maximum separation between a virtual and real drifter within the same grid cell is around 35 km. Hence, for separation distances larger than 35 km they are residing in different grid cells whereby they may become exposed to different velocity fields.

Using this information, the 1041 simulations had an estimated mean time for the drifter pairs to reach this separation of 35 km in 78 h (Table 2). The estimated separation velocity is in good agreement with the results from a global Finite-Scale Lyapunov Exponent analysis (Corrado et al., 2017), who estimate a mean separation velocity of the order of ~O(10 − 1)day-1 (~97 h to reach a 35 km separation) in the North Atlantic, which they ascribe to the presence of the Gulf Stream, a western boundary current with similar characteristics to the Agulhas Current. The only two regions that had an estimated mean time that was greater than that of the overall mean was the Benguela Upwelling System (104 h) and the Agulhas Return Current (116 h) (Fig. 8b). Not surprisingly, the shortest time of 35 h was found in the Agulhas Current region which was expected due to the intense currents. In contrast, it takes 55 h for the pairs to separate 35 km in the Agulhas Retroflection and 44 h in the Mozambique C. In comparison, Barron et al. (2007) reported separation distances between virtual and real drifters over one day to be about 25 km in the Agulhas Current, 25 km in the Mozambique Channel and ~15 km in the Benguela Upwelling System from simulations done in 2003. When compared to the work done in this paper, the mean separation distances between virtual and real drifters over one day was found to be 18 km in the Agulhas Current, 15 km in the Mozambique Channel and 9 km in the Benguela Upwelling System for the period between 1993 and 2015.

Barron et al. (2007) used NCOM (The Navy Coastal Ocean Model) which is a global ocean-prediction system that operates at a spatial resolution of 1/8° (12.5 km) and a three-hourly temporal resolution. NCOM assimilates near-real-time observational data from multiple sources including satellites, ships, floats and gliders (Mask and Bub, 2009). In comparison, the simulations run using the GlobCurrent-derived ocean product were found to be around 25% more accurate than the NCOM simulations reported by Barron et al. (2007). This suggests that the GlobCurrent-derived ocean current predictions are more accurate in spite the fact that the spatial resolution is courser.

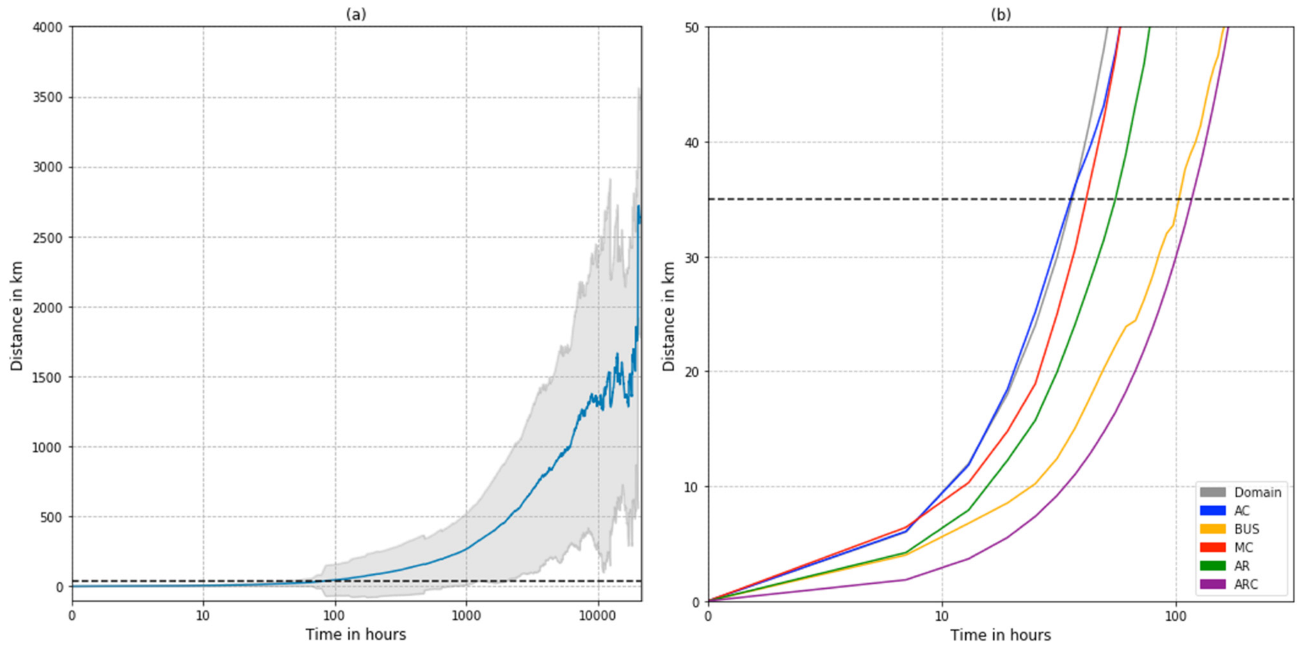

Fig. 8. Comparison of the overall distance between real and virtual drifters for the entire domain (2°W–70°E; 5–52°S) (left) and a regional comparison of the initial distance between real and virtual drifters (right). The blue line in the domain plot illustrates the mean distance between real and virtual drifters over time. The grey envelope surrounding the blue line is a representation of the standard deviation over time. The black dotted line in both illustrations represents 35 km distance between the real and virtual drifters. (For interpretation of the references to colour in this figure legend, the reader is referred to the web version of this article.)

Table 2
Summary of the all the observed drifter and virtual drifter runs for the full domain and the individual regions. The 2nd column specifies the number of real and virtual drifters that were deployed. The 3rd and 4th column specify the number of real drifters and virtual drifters that pass through the region. The 5th column refers to the time in hours that it takes for the separation distance between real and virtual drifters to reach 35 km.

Region	Drifters deployed within	Real drifters that pass through	Virtual drifters that pass through	35 km in hours
Full domain	1041	1041	1041	78
Agulhas Current	15	52	39	35
Benguela Upwelling System	36	70	63	104
Agulhas Retroflection	20	85	83	55
Mozambique Channel	30	67	65	44
Agulhas Return Current	54	151	154	116

4. Application of GlobCurrent virtual drifters in search and rescue operations

In this section, the virtual drifter trajectory simulations forced by GlobCurrent-derived current fields at 15 m depth is invoked in search and rescue applications. Two real-life experiments were conducted comparing observations with simulations.

4.1. Capsized catamaran off cape recife

Based on the approximate coordinates of a catamaran that was spotted off Cape Recife on the 18th of January 2016 and later salvaged by the NSRI (National Sea Rescue Institute) south of Cape Agulhas on the 23rd of January 2016 (Straton, 2016), a test experiment was conducted. 10,000 virtual drifters were deployed in a 1° × 1° resolution grid centred around the capsize location for 30-days (Fig. 9a). Disappointingly it was found that not even after 30 days did any of the virtual drifters make it to the approximate position where the capsized catamaran was salvaged by the NSRI five days later. However, the drift characteristics of the capsized catamaran are expected to be quite different from the virtual drifter simulations forced by the 15 m deep current. For example, the capsized catamaran was found breaching the sea surface and, therefore, its drift was most likely also affected by the direct drag exerted on the "aired" part of the catamaran structure by the near surface winds. The GlobCurrent-based simulations was not accounting for such affects. Hence, the simulated trajectories displayed inabilities to reach the location where the catamaran was salvaged.

The divergence error estimation derived in Section 3 provides the growth of the distance uncertainty over time. This is added to the virtual drifter trajectory as shown in Fig. 9b. The corresponding envelope covers the regions where the vessel could potentially be located using the synthetic particle tracking tool. As noticed the envelope just barely touched the observed location of the capsized vessel after 18 days. This is rather encouraging; although the simulation cannot accurately predict the trajectory of a capsized catamaran as explained above.

4.2. Drifter 109207

In order to assess the quality of the simulated drifter trajectories with limited direct wind drag contribution, a second simulation experiment was conducted using one real surface drifter drogued at 15 m (drifter number 109207). This drifter passed through the same region as the capsized catamaran but at a different time (5th August 2012). After deploying the 10,000 virtual drifters in the 1° × 1° grid around the starting location and comparing it to the drifter trajectory for 30 days (Fig. 10a), it was found that the GlobCurrent forced synthetic particle tracker provided trajectories in better agreement with the observed drifter. However, the real drifter displays a large looping pathway that only a few of the 10,000 simulations encounter.

This finding clearly demonstrates the need to use a large number of virtual drifters when making simulations of the trajectory of a real drifter, and is consistent with Barron et al. (2007) who emphasized that the simulation of drifter fate might be better represented as a probability distribution from a cluster of simulated drifters, each deployed

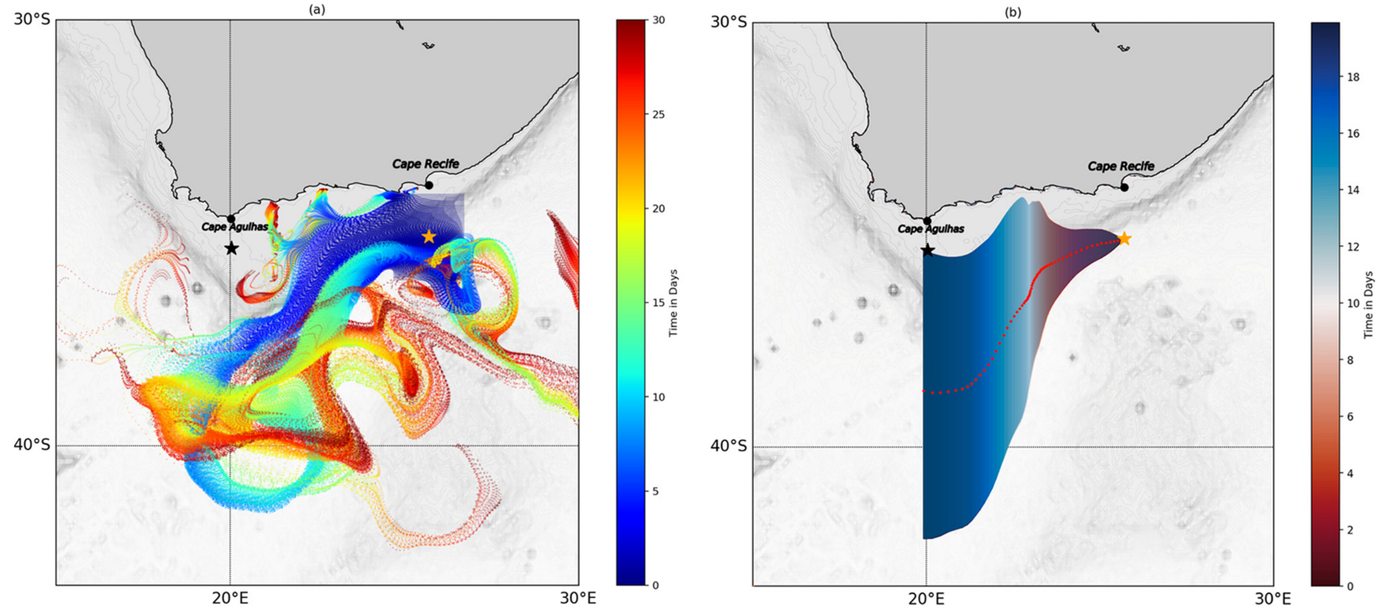

Fig. 9. The simulation of (a) 10,000 virtual drifters deployed for 30 days in a 1° × 1° grid centred around the starting location (orange star) of a capsized vessel and (b) a single virtual drifter (red) deployed for 18 days at the same starting location as the capsized vessel with an error probability area which indicates the mean error over time between simulations and observations in the Agulhas Current. The black star represents the final location of the capsized vessel. (For interpretation of the references to colour in this figure legend, the reader is referred to the web version of this article.)

at slightly different starting locations. Moreover, as noticed in Fig. 10b, a single virtual drifter deployed at the exact same location as the drifter provided a promising result. The entire observed drifter trajectory remained within the synthetic particle tracker uncertainty envelope with the virtual trajectory remaining in close proximity of the real drifter over the entire 18-day period.

Surface drifters drogued 15 m from the GDP are not directly affected by surface winds, which suggests that GlobCurrent is an appropriate tool for predicting trajectories of in-ocean objects, that are not exposed to surface winds. These drifters are, however, indirectly affected by the wind through the Ekman current which is incorporated into GlobCurrent. However, it remains difficult to conclude on this, since the dynamics in the region were significantly different between the two experiments.

5. Summary and conclusion

In this study, the combined geostrophic and Ekman current product at 15 m depth derived from the GlobCurrent repository has been used to compute and compare simulated virtual drifter trajectories with surface

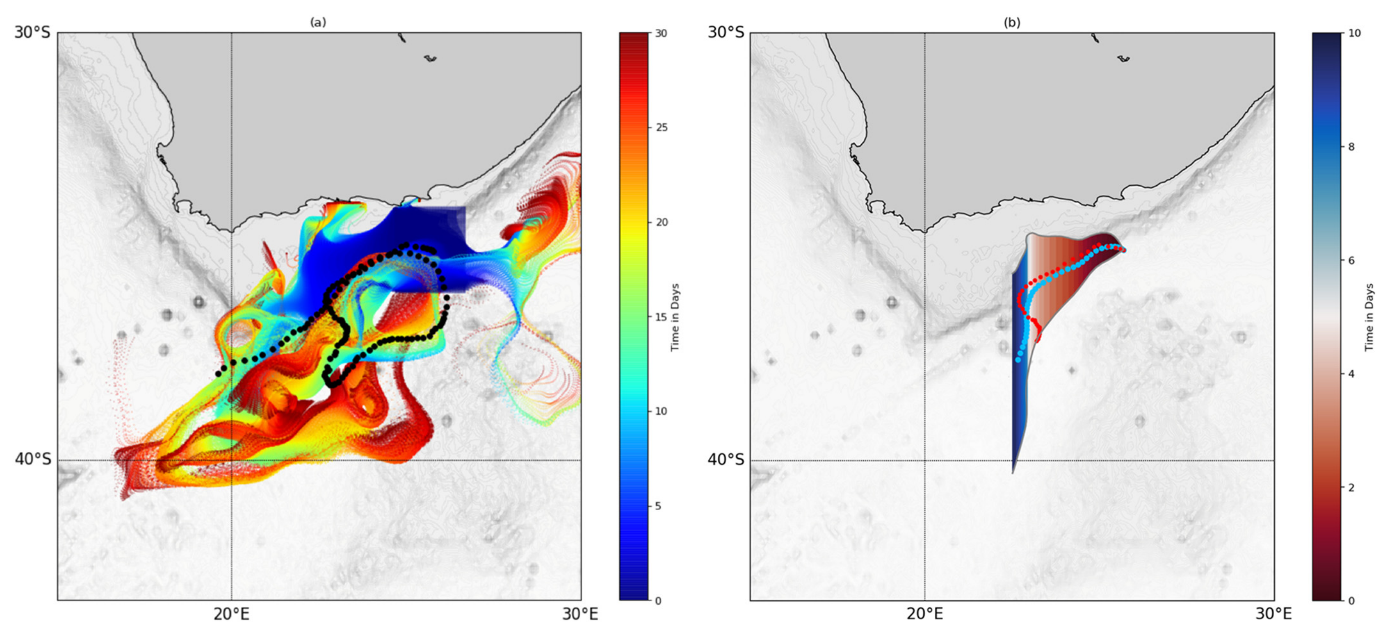

Fig. 10. The simulation of 10,000 virtual drifters deployed for 30 days in a 1° × 1° grid centred around the starting location of a capsized vessel (a). A single virtual drifter deployed for 10 days at the same starting location as the capsized vessel with an error probability area which indicates the mean error over time between simulations and observations in the Agulhas Current (b). The black line in (a) represents the trajectory of the drifter for 30 days. The red line and blue line in (b) represents the trajectory of the real drifter and virtual drifter respectively over 10 days. (For interpretation of the references to colour in this figure legend, the reader is referred to the web version of this article.)

drifting buoys drogued at 15 m in the Greater Agulhas Current Region. A total of 1041 drifters from 1993 to 2015 have been used. Gridded (50 km resolution) velocity maps of the mean virtual and observed drifters reveal fairly good agreement, in particular in the Agulhas Current, in the retroflection region and the Agulhas Return Current. However, in general the GlobCurrent products underestimate the velocity and sometimes also introduces disagreement in the drift-direction. This is also reported by Danielson et al., (in this issue). This underestimation results in the real and virtual drifter trajectories varying over time. The mean difference between all the simulated and observed velocities reveals that the GlobCurrent-based current field underestimated the ocean velocity by 27% throughout the entire domain. Regionally, the Agulhas Current has a mean variation of about 27%, the Benguela Upwelling System 64%, the Agulhas Retroflection 5%, the Mozambique Channel 35% and the Southern Ocean 11%.

The discrepancies in the velocities and drift paths are also invoking divergences between the virtual and real drifters that can reach > 35 km within 78 h. The simulations have a relatively course spatial resolution (25 km) and as such it is anticipated that the real and virtual drifters are exposed to different dynamics that can account for such a separation. Compared to previous studies in the same region (Barron et al., 2007), on the other hand, the GlobCurrent forced virtual drift trajectories were found to be 25% more reliable.

Using the virtual versus real drifter divergence information, we developed a divergence error envelope for the virtual drifter to estimate the virtual drifter spread. The divergence error envelope was applied to two simulation experiments where we examined the use of the GlobCurrent forced synthetic particle tracking tool in search and rescue applications. It was found that the GlobCurrent virtual drifters are not able to predict the trajectory of a capsized catamaran. It was concluded that this is most likely related to the drag characteristics and exposure of the above surface parts of the catamaran to the near surface wind. Provided this effect can be ignored and the drift characteristics are more strongly dependent on in-ocean currents, on the other hand, the particle tracker tool and simulations of drifter trajectories ensured useful information on drift speed and trajectories in terms of application for search and rescue.

In summary, the use of the synthetic particle tracking tool is promising for studies of upper ocean dynamics, although clearly constrained by apparent weaknesses in the GlobCurrent-based current products when it comes to search and rescue applications. In particular, the altimeter-based geostrophic current estimates lack sufficient spatial and temporal resolution. In turn, processes and dynamics at the mesoscales < 30 km and 3 days are not adequately resolved. Moreover, uncertainties in the Ekman currents are expected to exist from improper knowledge of the mixed layer depth and Ekman depth and their range of variabilities in this highly dynamic current regime.

However, recently Rio et al. (2016) and Rio and Santoleri (in this issue) revealed that the quality of the GlobCurrent-based merged geostrophic and Ekman current products can be improved by a dedicated sea surface height (SSH) to sea surface temperature (SST) correlation analyses. Compared to drifting buoy velocities these studies demonstrate that the SST data brings useful information on the surface currents in areas of strong SST gradients. Although further validation is needed before this new and refined dataset will be released, this is expected to strengthen the reliability of the GlobCurrent-based simulation of virtual drifter trajectories in areas like the Greater Agulhas Current Region. As such it will advance studies of ocean currents in areas of intense upper ocean dynamics and become highly valuable for model validations. Routine access to range Doppler velocity retrievals from the Sentinel-1 SAR missions may become an additional highly important contribution. Finally, with the launch of the SWOT mission in 2021 (https://swot.jpl.nasa.gov/mission.htm) detection of upper ocean mesoscale features with significantly finer resolution will also emerge and thus strengthen the observation-based framework for studies of mesoscale upper ocean dynamics.

Acknowledgements

The surface drifter data were downloaded from Atlantic Oceanographic & Meteorological Laboratory (www.aoml.noaa.gov) and are supplied by the Global Drifter Programme. The GlobCurrent velocity data are available at www.globcurrent.org We would like to thank the editor and the anonymous reviewers for their useful comments which have helped to improve the manuscript. We would also like to thank Mrs. Megan Andrews who gave valuable input about the design of a couple of the figures.

References

Ansorge, I.J., Lutjeharms, J.R.E., Best, P., Folkens, P.A., 2007. The Cetacean environment off Southern Africa. In: Whales and Dolphins of the Southern African subregion. Cambridge University Press, pp. 1–13.

Ansorge, I.J., Baringer, M.O., Campos, E.J.D., Dong, S., Fine, R.A., Garzoli, S.L., Goni, G., Meinen, C.S., Perez, R.C., Piola, A.R., Roberts, M.J., Speich, S., Sprintall, J., Terre, T., van den Berg, M.A., 2014. Basin-wide oceanographic array bridges the South Atlantic. Eos. Trans. AGU 95 (6), 53–60.

Backeberg, B.C., Johannessen, J.A., Bertino, L., Reason, C.J., 2008. The greater Agulhas Current system: an integrated study of its mesoscale variability. J. Oper. Oceanogr. 1 (1), 29–44.

Barron, C.N., Smedstad, L.F., Dastugue, J.M., Smedstad, O.M., 2007. Evaluation of ocean models using observed and simulated drifter trajectories: impact of sea surface height on synthetic profiles for data assimilation. J. Geophys. Res. 112, 1–12.

Beal, L.M., De Ruitjer, W.P.M., Biastoch, A., Zahn, R., 2011. On the role of the Agulhas system in ocean circulation and climate. Nature 472, 429–436.

Biastoch, A., Durgadoo, J.V., Morrison, A.K., van Sebille, E., Weijer, W., Griffies, S.M., 2015. Atlantic multi-decadal oscillation covaries with Agulhas leakage. Nat. Commun. 6, 1–7 (BB).

Blanke, B., Roy, C., Penven, P., Speich, S., McWilliams, J., Nelson, G., 2002. Linking wind and interannual upwelling variability in a regional model of the southern Benguela. Geophys. Res. Lett. 29 (41), 1–4.

Brambilla, E., Talley, L.D., 2006. Surface drifter exchange between the North Atlantic subtropical and subpolar gyres. J. Geophys. Res. 111, 1–16.

Corrado, R., Lacorata, G., Palatella, L., Santoleri, R., Zambianchi, E., 2017. General characteristics of relative dispersion in the ocean. Sci. Rep. 7, 1–11.

Danielson, R.E., Johannessen, J.A., Rio, M.H., Quartly, G., Chapron, B., Collard, F. and Donlon, C. 2018 Exploitation of error correlation in a large analysis validation: GlobCurrent case study (In review).

De Ruijter, W.P.M., Biastoch, A., Drijfhout, S.S., Lutjeharms, J.R.E., Matano, R.P., Pichevin, T., van Leeuwen, P.J., 1999. Indian-Atlantic inter-ocean exchange: dynamics, estimation and impact. J. Geophys. Res. 104, 20885–20910.

Ducet, N., Le Traon, P.Y., Reverdin, G., 2000. Global high-resolution mapping of ocean circulation from TOPEX/Poseidon and ERS-1 and -2. J. Geophys. Res. 105, 19477–19498.

Duncombe Rae, C.M., 1991. Agulhas retroflection rings in the South Atlantic Ocean: an overview. S. Afr. J. Mar. Sci. 11 (1), 327–344.

Elipot, S., Lumpkin, R., Perez, R.C., Lilly, J.M., Early, J.J., Sykulski, A.M., 2016. A global surface drifter data set at hourly resolution. J. Geophys. Res. Oceans 121 (5), 2937–2966.

Fredj, E., Carlson, D.F., Amitai, Y., Gozolchiani, A., Gildor, H., 2016. The particle tracking and analysis toolbox (PaTATO) for Matlab. Limnol. Oceanogr. Methods 14, 586–600.

Garzoli, S.L., Gordon, A.L., Kamenkovich, V., Pillsbury, D., Duncombe-Rae, C., 1996. Variability and sources of the south eastern Atlantic circulation. J. Mar. Res. 54, 1039–1071.

Gründlingh, M.L., 1983. On the course of the Agulhas current. S. Afr. Geogr. J. 65, 49–57.

Halo, I., Penven, P., Backeberg, B., Ansorge, I., Shillington, F., Roman, R., 2014a. Mesoscale eddy variability in the southern extension of the East Madagascar Current: seasonal cycle energy conversion terms and eddy mean properties. J. Geophys. Res. Oceans 119, 1–33.

Halo, I., Backeberg, B., Penven, P., Ansorge, I., Reason, C., Ullgren, J.E., 2014b. Eddy properties in the Mozambique Channel: a comparison between observations and two numerical ocean circulation models. Deep-Sea Res. 100, 38–53.

Hansen, D., Poulain, P.M., 1996. Quality control and interpolations of WOCE-TOGA drifter data. J. Atmos. Ocean. Technol. 13, 900–909.

Hardman-Mountford, N.J., Richardson, A.J., Agenbag, J.J., Hagen, E., Nykjaer, L., Shillington, F.A., Villacastin, C., 2003. Ocean climate of the South-East Atlantic observed from satellite data and wind models. Prog. Oceanogr. 59, 181–221.

Harris, T.F.W., Legeckis, R., van Foreest, D., 1978. Satellite infra-red images in the Agulhas Current system. Deep-Sea Res. 25, 543–548.

Hidalgo, M., Gusdal, Y., Dingsør, G.E., Ciannelli, L., Hjermann, D., Ottersen, G., Stige, L.C., Fossum, I., Melsom, A., Stenseth, N.C., 2009. Combining hydrographical particles-tracking models with spatial analyses to evaluate spatial dynamics of cod larvae and 0-group in the Barents Sea. ICES 6, 1–21.

Johannessen, J.A., Chapron, B., Collard, F., Rio, M.-H., Piollé, J.-F., Gaultier, L., Quartly, G., Shutler, J., Escola, R., Raj, R.P., Donlon, C., Danielson, R., Korosov, A., Nencioli, F., Kudryavtsev, V., Roca, M., Tournadre, J., Larnicol, G., Guitton, G., Miller, P., Warren, M., Hansen, M.W., 2016. GlobCurrent: Multisensor synergy for surface current estimation. In: Proceedings of Living Planet Symposium 2016, SP-740.

Krug, M., Tournadre, J., Dufois, F., 2014. Interactions between the Agulhas Current and

the eastern margin of the Agulhas Bank. Cont. Shelf Res. 81, 67–79.
Krug, M., Swart, S., Gula, J., 2017. Submesoscale cyclones in the Agulhas current. Geophys. Res. Lett. 44, 1–9.
Lange, M., van Sebille, E., 2017. Parcels v0.9: prototyping a Lagrangian ocean analysis framework for the petascale age. Geosci. Model Dev. 10, 4175–4186.
Lumpkin, R., Pazos, M., 2005. Measuring surface currents with Surface Velocity Program drifters: the instrument, its data and some recent results. In: Lagrangian Analysis and Prediction of Coastal and Ocean Dynamics, pp. 39–67.
Lumpkin, R., Grodsky, S.A., Centurioni, L., Rio, M.H., Carton, J.A., Lee, D., 2013. Removing spurious low-frequency variability in drifter velocities. J. Atmos. Ocean. Technol. 30, 353–360.
Lutjeharms, J.R.E., 2006. The Agulhas Current. Springer.
Lutjeharms, J.R.E., Ansorge, I.J., 2001. The Agulhas Return Current. J. Mar. Syst. 30, 115–138.
Lutjeharms, J.R.E., Valentine, H.R., 1988. Eddies at the sub-tropical convergence south of Africa. J. Phys. Oceanogr. 18, 761–774.
Lutjeharms, J.R.E., van Ballegooyen, R.C., 1988. The retroflection of the Agulhas Current. J. Phys. Oceanogr. 19, 1570–1583.
Lutjeharms, J.R.E., Boebel, O., Rossby, H.T., 2003. Agulhas cyclones. Deep-Sea Res. 50 (1), 13–34.
MacDonald, N.J., Davies, M.H., Zundel, A.K., Howlett, J.D., Demirbilek, Z., Gailani, J.Z., Lackey, T.C., Smith, J., 2006. PTM: Particle Tracking Model. US Army Corps of Engineers, Washington DC.
Mask, A.C., Bub, F., 2009. Skill Assessments of the Navy Coastal Ocean Model (NCOM) at the Naval Oceanographic Office.
McClean, J.L., Poulain, P.M., Pelton, J.W., Maltrud, M.E., 2002. Eulerian and Lagrangian statistics from surface drifters and a high-resolution POP simulation in the North Atlantic. J. Phys. Oceanogr. 32, 2472–2791.
Meyer, I., Braby, L., Krug, M., Backeberg, B., 2017. Mapping the ocean current strength and persistence in the Agulhas to inform marine energy development. Mar. Renew. Energy 179–215.
Morris, T., Hermes, J., Beal, L., du Plessis, M., Duncombe Rae, C., Gulekana, M., Lamont, T., Speich, S., Roberts, M., Ansorge, I.J., 2017. The importance of monitoring the Greater Agulhas Current and its inter-ocean exchanges using large mooring arrays. S. Afr. J. Sci. 113 (7/8), 1–7.
Qin, X., van Sebille, E., Gupta, A.S., 2014. Quantification of errors induced by temporal resolution on Lagrangian particles in an eddy-resolving model. Ocean Model 76, 20–30.
Rio, M.-H., Santoleri, R., 2018. Improved global surface currents from the merging of altimetry and Sea Surface Temperature data. Remote Sens. Environ (this issue).
Rio, M.H., Mullet, S., Picot, N., 2014. Beyond GOCE for the ocean circulation estimate: synergetic use of altimetry, gravimetry, and in-situ data provides new insight into geostrophic and Ekman currents. Geophys. Res. Lett. 41 (24), 8918–8925.
Rio, M.-H., Santoleri, R., Bourdalle-Badie, R., Griffa, A., Piterbarg, L., Taburet, G., 2016. Improving the altimeter derived surface currents using high-resolution sea surface temperature data: a feasibility study based on model outputs. J. Atmos. Ocean. Technol. 33. http://dx.doi.org/10.1175/JTECH-D-16-0017.1.
Rouault, M.J., Mouche, A., Collard, F., Johannessen, J.A., Chapron, B., 2010. Mapping the Agulhas Current from space: an assessment of ASAR surface current velocities. J. Geophys. Res. 115, 1–14.
Rubio, A., Blanke, B., Speich, S., Grima, N., Roy, C., 2009. Mesoscale eddy activity in the southern Benguela upwelling system from satellite altimetry and model data. Prog. Oceanogr. 83, 288–295.
Saraceno, M., Strub, P.T., Kosro, P.M., 2008. Estimates of sea surface height and near-surface alongshore coastal currents from combinations of altimeters and tide gauges. J. Geophys. Res. 113, 1–20.
Sayol, J.M., Orfila, A., Simarro, G., Conti, D., Renault, L., Molcard, A., 2013. A Lagrangian model for tracking surface spills and SaR operations in the ocean. Environ. Model. Softw. 52, 74–82.
Speich, S., Arhan, M., Rusciano, E., Faure, V., Ollitrault, M., Prigent, A., Swart, S., 2012. Use of Argo Floats to study the ocean dynamics south of Africa: what we have learned from the Goodhope project and what we plan within the SAMOC International Programme. Mercator Ocean-Coriolis Q. Newsl. 45, 21–27.
Straton, A., 2016. Tragic capsized catamaran drifts past Port Elizabeth. MyPE News (Available). www.mype.co.za/new/tragic-capsized-catamaran-drifts-past-port-elizabeth/59957/2016/01, Accessed date: 20 January 2018.
Thorpe, S.E., Heywood, K.J., Stevens, D.P., Brandon, M.A., 2004. Tracking passive drifters in a high-resolution ocean model: implications for interannual variability of larval krill transport to South Georgia. Deep-Sea Res. I Oceanogr. Res. Pap. 51, 909–920.
Van der Lingen, C.D., Shannon, L.J., Cury, P., Kreiner, A., Moloney, C.L., Roux, J.P., Vaz-Velho, F., 2006. Resource and ecosystem variability, including regime shifts, in the Benguela Current System. Large Mar. Ecosyst. 14, 147–184.
Van Leeuwen, P.J., de Ruijter, W.P.M., Lutjeharms, J.R.E., 2000. Natal Pulses and the formation of Agulhas Rings. J. Geophys. Res. 105, 6425–6436.
Van Sebille, E., van Leeuwen, P.J., Biastoch, A., de Ruitjer, W.P.M., 2010. On the fast decay of Agulhas rings. J. Geophys. Res. 115, 1–15.
Van Sebille, E., Griffies, S.M., Abernathey, R., Adams, T.P., Berloff, P., Biastoch, A., Blanke, B., Chassignet, E.P., Cheng, Y., Cotter, C.J., Deleersnijder, E., Döös, K., Drake, H.F., Drijfhout, S., Gary, S.F., Heemink, A.W., Kjellsson, J., Koszalka, I.M., Lange, M., Lique, C., MacGilchrist, G.A., Marsh, R., Adame, C.G.M., McAdam, R., Nencioli, F., Paris, C.B., Piggott, M.D., Polton, J.A., Rühs, S., Shah, S.H.A.M., Thomas, M.D., Wang, J., Wolfram, P.J., Zanna, L., Zika, J.D., 2018. Lagrangian ocean analysis: fundamentals and practices. Ocean Model 121, 49–75.
Xu, J., Lowe, R.J., Ivey, G.N., Jones, N.L., Zhang, Z., 2016. Ocean transport pathways to a world heritage fringing coral reef: Ningaloo reef, western Australia. PLoS 11 (1), 1–26.
Zheng, S., Du, Y., Li, J., Cheng, X., 2015. Eddy characteristics in the South Indian Ocean as inferred from surface drifters. Ocean Sci. J. 11, 361–371.